

ZAMM · Z. angew. Math. Mech. 95 (1995) 10, 783–799

Akademie Verlag

JÜNGEL, A.

Numerical Approximation of a Drift-Diffusion Model for Semiconductors with Nonlinear Diffusion

Diese Arbeit beschäftigt sich mit der numerischen Approximation des transienten, eindimensionalen Drift-Diffusions-Modells, das aus einer Poisson-Gleichung für das elektrische Potential und zwei nichtlinearen Zustandsgleichungen für die Leiterdichten besteht. Die nichtlinearen Diffusionsterme sind so geartet, daß die parabolischen Gleichungen degeneriert sind. Wir zeigen, daß die Gleichungen transiente Lösungen erlauben, für die die Leiterdichten lokal verschwinden.

Nachdem wir uns ein Existenz- und Eindeutigkeitsresultat ins Gedächtnis gerufen und die Regularität der Lösungen bewiesen haben, diskretisieren wir die Gleichungen mittels der Methode der exponentiellen Anpassung und geben Beispiele von Vakuumlösungen an. Wir zeigen numerisch, daß Vakuumlösungen auch dann auftreten, wenn eine physikalisch sinnvolle PN-Übergangsdioden betrachtet wird. Infolge des Vakuumeffekts ändert sich das Wachstum der statischen Strom-Spannungs-Charakteristik für eine Durchlaßvorspannungs-Diode an der sogenannten Schwellenspannung. Im hohen Einschuß-Regime der Durchlaßvorspannungs-Diode erweist sich das Wachstum der Charakteristik als polynomial.

This paper is concerned with the numerical approximation of the transient, one-dimensional drift-diffusion model consisting of a Poisson equation for the electric potential and two nonlinear continuity equations for the carrier densities. The nonlinear diffusion terms are such that the parabolic equations are of degenerate type. We show that the equations admit transient solutions for which the carrier densities vanish locally. These solutions are called vacuum solutions.

After recalling an existence and uniqueness result and proving the regularity of the solutions, we discretize the equations using the mixed exponential fitting method and present examples of vacuum solutions. We show numerically that vacuum solutions also occur if a physically reasonable PN junction diode is considered. Due to the vacuum effect the growth of the static voltage-current characteristic for a forward biased diode changes at the so-called threshold voltage. In the high injection regime of the forward biased diode the growth of the characteristic turns out to be polynomial.

MSC (1991): 35K57, 35J05, 65N22, 76R50, 78A30

1. Introduction

1.1. In this paper we consider the following one-dimensional drift-diffusion model for a bipolar semiconductor:

$$qn_t - (J_n)_x = -qR(n, p), \quad J_n = q(D_n r(n)_x - \mu_n n V_x), \quad (1.1)$$

$$qp_t + (J_p)_x = -qR(n, p), \quad J_p = -q(D_p r(p)_x + \mu_p p V_x), \quad (1.2)$$

$$\varepsilon V_{xx} = q(n - p - C) \quad \text{in } I = (0, l), \quad (1.3)$$

where $n_t = \partial n / \partial t$, $(J_n)_x = \partial J_n / \partial x$, etc. Here n , J_n denote the electron density and the electron current, respectively. p , J_p are the analogously defined physical quantities of the positively charged holes. r is the pressure, V the electric potential, and $C = C(x)$ the prescribed doping profile characterizing the device under consideration. D_n , D_p are the diffusion coefficients for the electrons and holes, resp., μ_n , μ_p are the corresponding mobilities, q denotes the elementary charge and ε the permittivity constant of the device. For physical reasons we require n , p , r , $r' \geq 0$. $R = R(x, t, n, p)$ denotes the recombination-generation rate. The functions n , p and V depend on the spatial variable $x \in I$ and on the time variable $t \geq 0$, where $I \in \mathbb{R}$ is the (bounded) semiconductor domain.

Equations (1.1)–(1.3) can be obtained as limit of the hydrodynamic model for a bipolar semiconductor as the electron and hole mean free paths tend to zero (see [18], [19]).

We have assumed that the electrons and holes behave – thermodynamically spoken – as ideal gases, i.e., the electron and hole pressure is given by

$$r(s) = sT(s).$$

Here T is the temperature which is assumed to be the same function for the electrons and the holes. The usual considerations on which the isentropic hydrodynamic model is based suggest a pressure function of the form [7]

$$r(s) = s^\alpha, \quad \alpha = \frac{5}{3}. \quad (1.4)$$

The recombination-generation rate is of the form

$$R(n, p) = G(n, p) - F(n, p),$$

where G denotes the recombination rate and F the generation term.

We supplement these equations with Dirichlet boundary conditions [17]:

$$n = n_D, \quad p = p_D, \quad V = V_D \quad \text{on } \partial I. \quad (1.5)$$

∂I models the union of Ohmic contacts. We assume that the densities at time $t = 0$ are known:

$$n(x, 0) = n_I, \quad p(x, 0) = p_I \quad \text{a.e. in } I. \quad (1.6)$$

The name drift-diffusion model originates from the type of dependence of the current densities J_n, J_p on the carrier densities n, p and the electric field $-V_x$. The current densities are the sums of the drift terms $-\mu_n n V_x, -\mu_p p V_x$ and diffusion terms $D_n r(n)_x, -D_p r(p)_x$.

1.2. In [11] existence and (under some conditions) uniqueness of multi-dimensional solutions of (1.1)–(1.6) is shown. We recall these results in Section 2 and prove that $n^{(\alpha+1)/2}, p^{(\alpha+1)/2} \in H^1((0, l) \times (0, T))$ if homogeneous Dirichlet condition are prescribed.

It is well known that the discretization of the standard drift-diffusion model, i.e. the model with linear pressure does not give good results if it is carried out in the standard way [22]. This is caused by very large values of $|V_x|$ at the PN junctions where the doping profile changes sign. We use therefore the mixed exponential fitting method described in [4, 1, 5, 29] to overcome this difficulty. This method is adapted to the model with nonlinear diffusion in Section 3.

Numerical results showing the transient behaviour of the solutions are presented in Section 4. It turns out that vacuum only occurs for $t < t_0$ where $t_0 > 0$ and in the limit $t \rightarrow \infty$ if the steady state is in thermal equilibrium.

In Section 5 we model a PN junction diode. For this purpose we compute the diffusion coefficients and scale the equations appropriately. We numerically show that there are vacuum solutions for all $t \geq 0$ in the case of a reverse and slightly forward biased junction.

In Section 6 we compute static voltage-current characteristics of a diode and show that the total current $J = J_n + J_p$ vanishes in the reverse direction as well as in the forward direction for applied small voltages U not exceeding the so-called threshold voltage U_{th} (since due to the vacuum no current can flow). The dependence of the current on the applied voltage $U > U_{th}$ appears to be polynomial. The numerical values of U_{th} for a Si and Ge diode are of the same order as the experimental values.

This behaviour seems to be contradictory to the characteristic of the standard drift-diffusion model where J depends exponentially on U :

$$J = J_s(e^{U/U_T} - 1). \quad (1.7)$$

The Shockley equation (1.7), however, is only valid in the low injection regime (i.e. U not too large compared to the thermal voltage U_T), and under high injection conditions $U > 10U_T$ (for example) the growth of the characteristic slows down (cf. [24, Ch. 2.4.3], [19, Ch. 4.2]). Thus our numerical results can be interpreted to be valid in the high injection case.

2. Existence, uniqueness, and regularity

2.1. We consider the drift-diffusion model where the physical parameters are set to one:

$$n_t - (r(n)_x - nV_x)_x = -R(n, p) \quad \text{in } Q_T, \quad (2.1)$$

$$p_t - (r(p)_x + pV_x)_x = -R(n, p) \quad \text{in } Q_T, \quad (2.2)$$

$$V(t)_{xx} = n(t) - p(t) - C(x) \quad \text{in } I \quad \text{for a.e. } t \in (0, T), \quad (2.3)$$

$$n(0, t) = n_0(t), \quad n(l, t) = p_1(t), \quad (2.4)$$

$$p(0, t) = p_0(t), \quad p(l, t) = n_1(t), \quad (2.5)$$

$$V(0, t) = V_0(t), \quad V(l, t) = V_1(t) \quad \text{for a.e. } t \in (0, T), \quad (2.6)$$

$$n(x, 0) = n_I(x), \quad p(x, 0) = p_I(x) \quad \text{in } I, \quad (2.7)$$

where $I = (0, l)$, $l > 0$, and $Q_T = I \times (0, T)$, $T > 0$.

We impose the following hypotheses:

(H1) Pressure: $r \in C^1(\mathbb{R})$, $r(0) = r'(0) = 0$, $r'(s) \geq c_0 s^{\alpha-1}$ for all $s > 0$ for some $c_0 > 0$, $\alpha > 1$.

(H2) Data: $C \in L^\infty(I)$; $n_I, p_I \in L^\infty_+(I) \stackrel{\text{def}}{=} \{u \in L^\infty(I) : u \geq 0\}$; $n_0, n_1, p_0, p_1 \in H^1(0, T) \cap L^\infty_+(0, T)$, $V_0, V_1 \in L^\infty(0, T)$.

(H3) Recombination: Let $R: Q_T \times \mathbb{R}^2 \rightarrow \mathbb{R}$ be a function with $R(x, t, n, p) = G(x, t, n, p) - F(x, t, n, p)$, where $F \geq 0$ and G are Carathéodory functions of $(x, t) \in Q_T$ and $(n, p) \in \mathbb{R}^2$ (see, e.g. [26]), $G(x, t, \cdot, \cdot)$, $G(x, t, n, \cdot)$, $-F(x, t, \cdot, \cdot)$, $-F(x, t, n, \cdot)$ are nondecreasing, and $G(x, t, 0, p) = G(x, t, n, 0) = 0$.

For notational simplicity let here and in the following n_D, p_D, V_D be linear functions interpolating the Dirichlet boundary data in (2.4)–(2.6).

We have the following existence and uniqueness result [11].

Theorem 2.2: Let (H1)–(H3) hold and let $T > 0$.

Existence: There exists a generalized solution (n, p, V) of (2.1)–(2.7) such that

$$n, p \in L_+^\infty(Q_T) \cap H^1(0, T; H^{-1}(I)),$$

$$r(n), r(p) \in L^2(0, T; H^1(I)),$$

$$V \in L^\infty(0, T; H^2(I)).$$

Uniqueness: Suppose that R is locally Lipschitz continuous in (n, p) uniformly in (x, t) and $G(x, t, n, p) \leq c_1 np$ in $Q_T \times \mathbb{R}_+^2$ for some $c_1 \geq 0$. If

(i) $n_I, p_I \geq \gamma(T) > 0$ in I , $n_D, p_D \geq \gamma(T) > 0$ in $(0, T)$, or

(ii) $-\nabla V$ depends on the initial and boundary data but not on n and p ,

then the solution of (i) (2.1)–(2.7), and (ii) (2.1)–(2.2), (2.4)–(2.7), resp. is unique.

For the standard drift-diffusion model (i.e. with linear pressure), usually the Shockley-Read-Hall term $R(n, p) = g(n, p)(np - n_i^2)$ is taken as recombination-generation rate [19]. In thermal equilibrium $R(n_e, p_e) = 0$ must hold which implies $n_e p_e = n_i^2$. In the case of nonlinear pressure $r(s) = s^\alpha$, $\alpha > 1$, the thermal equilibrium condition $n_e p_e = n_i^2$ must be replaced by $n_e^{\alpha-1} + p_e^{\alpha-1} = \text{const.}$ (see [20]). Therefore, the Shockley-Read-Hall term cannot be taken if the pressure is nonlinear.

The hypothesis (H3) can be interpreted physically: The process of transferring an electron of the conduction band of the semiconductor into the lower energetic valence band is called *recombination of electron-hole pairs*. The inverse process, i.e. the transfer of a valence electron to the conduction band is termed *generation of electrons and holes*. If one of the densities vanishes no recombination can occur and we have $G(0, p) = G(n, 0) = 0$. High density concentrations prevent the generation of electron-hole pairs; on the contrary, the recombination rate increases as the densities increase. Therefore it is physically reasonable to suppose that $G(F)$ is a nondecreasing (nonincreasing) function in n and p .

Theorem 2.2 is also valid in the multi-dimensional case with mixed Dirichlet-Neumann boundary conditions (see [11] for details). Since the parabolic equations are degenerate (i.e. not uniformly parabolic), we cannot expect that the densities n and p lie in the space $L^2(0, T; H^1(I))$ [13]. In return we can show in the one-dimensional case that there is a solution satisfying $n, p \in L^2(0, T; C^0(\bar{I}))$.

Theorem 2.3: Let (H1)–(H2) hold. Suppose that $R = 0$, $n_D = p_D = 0$, $V_0, V_1 \in C^0([0, T])$, and $n_I, p_I \in H_0^1(I)$. Then there exists a solution of (2.1)–(2.7) such that

$$n^{(\alpha+1)/2}, p^{(\alpha+1)/2} \in H^1(Q_T), \quad r(n), r(p) \in L^\infty(0, T; H_0^1(I)). \quad (2.8)$$

Proof: We use an approximation argument to obtain appropriate a priori estimates. For this purpose let $M = M(T) > 0$ such that $n, p \leq M$ in Q_T , and let $C_\varepsilon \in C_0^\infty(I)$, $n_{I\varepsilon}, p_{I\varepsilon} \in C_0^\infty(I)$, $V_{0\varepsilon}, V_{1\varepsilon} \in C^\infty([0, T])$, and $r_\varepsilon \in C^2([0, M])$ such that

$$\begin{aligned} C_\varepsilon &\rightarrow C & \text{in } L^2(I), & \|C_\varepsilon\|_{0,\infty,I} \leq \|C\|_{0,\infty,I}, \\ n_{I\varepsilon} &\rightarrow n_I & \text{in } H_0^1(I), & \|n_{I\varepsilon}\|_{0,\infty,I} \leq \|n_I\|_{0,\infty,I}, \\ p_{I\varepsilon} &\rightarrow p_I & \text{in } H_0^1(I), & \|p_{I\varepsilon}\|_{0,\infty,I} \leq \|p_I\|_{0,\infty,I}, \\ V_{0\varepsilon} &\rightarrow V_0 & \text{in } C^0([0, T]), & \|V_{0\varepsilon}\|_{0,\infty,I} \leq \|V_0\|_{0,\infty,I}, \\ V_{1\varepsilon} &\rightarrow V_1 & \text{in } C^0([0, T]), & \|V_{1\varepsilon}\|_{0,\infty,I} \leq \|V_1\|_{0,\infty,I}, \\ r_\varepsilon &\rightarrow r & \text{in } C^0([0, M]), & r'_\varepsilon \geq r', \quad r_\varepsilon \geq r, \quad r_\varepsilon \geq \varepsilon \quad \text{in } [0, M]. \end{aligned}$$

From the results in [11] it follows that there exists a solution $(n_\varepsilon, p_\varepsilon, V_\varepsilon)$ of the problem (2.1)–(2.7) where the data are replaced by the approximate data defined above such that

$$n_\varepsilon, p_\varepsilon \in L_+^\infty(Q_T) \cap L^2(0, T; H^1(I)) \cap H^1(0, T; H^{-1}(I)),$$

$$V_\varepsilon \in L^2(0, T; H^2(I)).$$

Using the theorems in [14, p. 460, p. 459, p. 320] we find that $(n_\varepsilon, p_\varepsilon, V_\varepsilon)$ is a classical solution of (2.1)–(2.7) with $(n_\varepsilon)_{x\varepsilon}, (p_\varepsilon)_{x\varepsilon} \in L^2(Q_T)$. As in [11] it can be shown that $(n_\varepsilon, p_\varepsilon, V_\varepsilon)$ converges in $(L^2(Q_T))^2 \times L^2(0, T; H^1(I))$ to (n, p, V) which is a solution of the original problem (2.1)–(2.7). Furthermore, it holds

$$\int_{Q_T} r'_\varepsilon(n_\varepsilon) ((n_\varepsilon)_x)^2 \leq c, \quad (2.9)$$

where $c > 0$ here and in the following is a constant independent of ε .

Now use $r_\varepsilon(n_\varepsilon)_t \in L^2(0, T; H_0^1(I))$ as test function in (2.1). We get

$$\begin{aligned} \int_{Q_T} r'_\varepsilon(n_\varepsilon) ((n_\varepsilon)_t)^2 + \frac{1}{2} \int_{Q_T} \frac{d}{dt} (r_\varepsilon(n_\varepsilon)_x)^2 &= - \int_{Q_T} ((n_\varepsilon)_x (V_\varepsilon)_x + n_\varepsilon (V_\varepsilon)_{xx}) r'_\varepsilon(n_\varepsilon) (n_\varepsilon)_t \\ &\leq \frac{1}{2} \int_{Q_T} r'_\varepsilon(n_\varepsilon) ((n_\varepsilon)_t)^2 + c \int_{Q_T} r'_\varepsilon(n_\varepsilon) ((n_\varepsilon)_x)^2 + \int_{Q_T} n_\varepsilon^2 (n_\varepsilon - p_\varepsilon - C_\varepsilon)^2 r'_\varepsilon(n_\varepsilon) \end{aligned}$$

and thus

$$\int_{Q_T} r'_\varepsilon(n_\varepsilon) ((n_\varepsilon)_t)^2 + \int_I (r_\varepsilon(n_\varepsilon)_x(t))^2 \leq \int_I (r'_\varepsilon(n_\varepsilon) (n_\varepsilon)_{I\varepsilon})^2 + c \leq c.$$

Set $F_\varepsilon(u) = \int_0^u \sqrt{r'_\varepsilon(s)} ds$ for $u \geq 0$. Since

$$r'_\varepsilon(n_\varepsilon) ((n_\varepsilon)_t)^2 = \left(\frac{d}{dt} F_\varepsilon(n_\varepsilon) \right)^2$$

we obtain the estimates

$$\|r_\varepsilon(n_\varepsilon)\|_{L^\infty(0, T; H^1(I))} \leq c, \quad \|F_\varepsilon(n_\varepsilon)\|_{H^1(0, T; L^2(I))} \leq c.$$

We conclude that

$$\begin{aligned} r_\varepsilon(n_\varepsilon) &\overset{*}{\rightharpoonup} r(n) \quad \text{in } L^\infty(0, T; H^1(I)), \\ F_\varepsilon(n_\varepsilon) &\rightharpoonup \int_0^n \sqrt{r'(s)} ds \quad \text{in } H^1(0, T; L^2(I)). \end{aligned}$$

From (H1) we find

$$n^{(\alpha+1)/2} \leq \frac{\alpha+1}{2\sqrt{c_0}} \int_0^n \sqrt{r'(s)} ds$$

which, together with (2.9), gives $n^{(\alpha+1)/2} \in H^1(Q_T)$. \square

Remark 2.4: The regularity result (2.8) is also valid in the multi-dimensional case if homogeneous Dirichlet boundary conditions are prescribed and the boundary of the semiconductor domain is of class $C^{2+\alpha}$ ($\alpha > 0$). Furthermore, the theorem remains valid for nonvanishing R if e.g., R is Hölder continuous in all variables.

3. Numerical approximation

3.1. In this Section we give a discretization scheme for the equations (2.1)–(2.7). SCHARFETTER and GUMMEL [22] proposed for the one-dimensional problem to treat the equations of the standard drift-diffusion model as differential equations in n and p with J_n , J_p , and V_x assumed constant between mesh points. In [1] the mixed exponential fitting method is adapted to a unipolar advection-dominated drift-diffusion model with nonlinear pressure. Mixed methods are described e.g. in [21, 4, 5]. The basic idea of this method is to write the continuity equations of the standard model as $(J_n)_x = (e^V w_n)_x$, $(J_p)_x = -(e^{-V} z_p)_x$ through the change of variables $w = n e^{-V}$, $z = p e^V$. We shall adapt this method to the nonlinear bipolar model.

We assume throughout this Section that

$$r(s) = s^\alpha, \quad s \geq 0, \quad \alpha > 1,$$

and we will neglect recombination-generation effects, that means we set $R(n, p) = 0$. Moreover, we assume that the boundary data are time-independent.

3.2. Time discretization. The problem (2.1)–(2.7) is solved via the explicit Euler method as follows: Let $t_j = j\tau$, $j \geq 0$, $k > 0$, and set

$$n^j = n(t_j), \quad p^j = p(t_j), \quad V^j = V(t_j), \quad j \geq 0.$$

Given n^0, p^0 verifying the boundary conditions (2.4)–(2.5) solve for $j \geq 0$:

$$\frac{n^{j+1} - n^j}{k} - (((n^j)^\alpha)_x - n^j(V^j)_x)_x = 0, \quad (3.1)$$

$$\frac{p^{j+1} - p^j}{k} - (((p^j)^\alpha)_x + p^j(V^j)_x)_x = 0, \quad (3.2)$$

$$(V^j)_{xx} = n^j - p^j - C \quad \text{in } (0, l) \quad (3.3)$$

subject to the boundary conditions (2.4)–(2.6). The Euler method has the disadvantage that k must be chosen very “small” compared to the mesh size h (more precisely $k/h^2 < 1$), but it is simple to implement and sufficient for our purpose.

3.3. Space discretization. As mentioned above we discretize the equations (2.1)–(2.2) via the mixed exponential fitting method. The Poisson equation (2.3) can be discretized using standard finite differences.

Let $x_i = ih$, where $h = l/N$, $i \geq 0$, $h > 0$, and set $I_i = (x_{i-1}, x_i)$, $i = 1, \dots, N$, and

$$n_i^j = n^j(x_i), \quad p_i^j = p^j(x_i), \quad V_i^j = V^j(x_i), \quad i = 0, \dots, N.$$

In the following we restrict our attention to the hole density in (3.2). Equation (3.1) can be discretized analogously.

We will discretize

$$J_p = -(r'(p)p_x + pV_x), \quad (J_p)_x = -f_k \quad \text{in } (0, l), \quad (3.4)$$

where $r'(p) = \alpha p^{\alpha-1}$ and $f_k = (p^{j+1} - p^j)/k$. Here and in the following the index j is omitted. The discretization is done in several steps.

First step: approximation of r' . We approximate $r'(p)$ with a piecewise constant function \bar{r} defined by

$$r'(p) \simeq \bar{r}, \quad \bar{r}|_{I_i} = r_i = \begin{cases} r'(p_{i-1}) & \text{if } J_p|_{I_i} > 0 \\ r'(p_i) & \text{if } J_p|_{I_i} \leq 0, \end{cases} \quad i = 1, \dots, N. \quad (3.5)$$

If the current J_p in I_i at time t_j is positive (negative) we expect that the holes flow in the direction of the right (left) interval point, thus we take the density value at the left (right) node p_{i-1} (p_i) as approximation in $r'(p)$. In this definition we need an approximation of the current (3.4) which we just want to discretize. To overcome this problem we use a simple approximation of J_p to define r_i , and using \bar{r} we find an improved discretization of J_p in the next steps.

Since in $\{p > 0\}$

$$J_p = -p \left(\frac{\alpha}{\alpha-1} p^{\alpha-1} + V \right)_x$$

we can complete the definition of \bar{r} in (3.5) by setting

$$\begin{aligned} J_p|_{I_i} &\simeq \bar{J}_{p,i}, \\ \bar{J}_{p,i} &= \begin{cases} 0 & \text{if } p_i = p_{i-1} = 0 \\ -h^{-1} \left(\frac{\alpha}{\alpha-1} (p_i^{\alpha-1} - p_{i-1}^{\alpha-1}) + (V_i - V_{i-1}) \right) & \text{else,} \end{cases} \end{aligned} \quad (3.6)$$

$i = 1, \dots, N$. The current J_p in (3.4) is then approximated by

$$J_p \simeq -(r_i p_x + p V_x) \quad \text{in } I_i, \quad i = 1, \dots, N.$$

Second step: change of variables. Using the change of variables,

$$z = p e^{V/r_i} \quad \text{in } I_i,$$

the expression for the current becomes

$$J_p \simeq -(r_i e^{-V/r_i} z_x) \quad \text{in } I_i.$$

If $r_i = 0$, then the current vanishes; thus in the following we assume $r_i > 0$. Equation (3.4) can be rewritten in terms of the variables J_p and z as:

Find $(z, J_p) \in L^2(I) \times H^1(I)$ such that

$$r_i^{-1} e^{V/r_i} J_p + z_x \simeq 0, \quad (3.7)$$

$$(J_p)_x = -f_k \quad \text{in } I_i. \quad (3.8)$$

Here V is given (from (3.3)) such that V_x is constant in I_i , $i = 1, \dots, N$. Multiplying (3.7) and (3.8) by test functions and integrating over all intervals gives the following formulation:

$$\sum_{i=1}^N \left[\int_{I_i} \frac{1}{r_i} e^{V/r_i} J_p \tau - \int_{I_i} z \tau_x + [p e^{V/r_i} \tau]_{x_{i-1}}^{x_i} \right] = 0, \quad (3.9)$$

$$\sum_{i=1}^N \int_{I_i} (J_p)_x \varphi = - \sum_{i=1}^N \int_{I_i} f_k \varphi, \quad (3.10)$$

$$\sum_{i=1}^{N-1} q(x_i) (J_p(x_i + 0) - J_p(x_i - 0)) = 0. \quad (3.11)$$

The equation (3.11) describes the continuity of J_p at the interval end points. Here τ is a piecewise regular function, $\varphi \in L^2(I)$ and q is defined at the nodes such that $q(0) = p_D(0)$, $q(l) = p_D(1)$.

Third step: the discrete system. Define

$$X_h = \{ \tau \in L^2(I) : \tau(x) = a_i x + b_i \text{ in } I_i, i = 1, \dots, N \},$$

$$W_h = \{ \varphi \in L^2(I) : \varphi \text{ is constant in } I_i, i = 1, \dots, N \},$$

$$M_h = \{ q \text{ defined at the nodes } x_0, \dots, x_N : q(0) = p_D(0), q(l) = p_D(1) \}.$$

We approximate

$$J_p \simeq J_p^h \in X_h, \quad z \simeq z^h \in W_h, \quad p \simeq p^h \in M_h, \quad V \in X_h.$$

The discrete system then consists of three equations for the three unknowns J_p^h , z^h , and p^h :

Find $J_p^h \in X_h$, $z^h \in W_h$, $p^h \in M_h$ such that

$$\sum_{i=1}^N \left[\int_{I_i} \frac{1}{r_i} e^{V/r_i} J_p^h \tau - \int_{I_i} z^h \tau_x + [p^h e^{V/r_i} \tau]_{x_{i-1}}^{x_i} \right] = 0, \quad (3.12)$$

$$\sum_{i=1}^N \int_{I_i} (J_p^h)_x \varphi = - \sum_{i=1}^N \int_{I_i} f_k \varphi, \quad (3.13)$$

$$\sum_{i=1}^{N-1} q(x_i) (J_p^h(x_i + 0) - J_p^h(x_i - 0)) = 0 \quad (3.14)$$

for $\tau \in X_h$, $\varphi \in W_h$, $q \in M_h$. Equations (3.12)–(3.14) can be recognized as the one-dimensional lowest order Raviart-Thomas mixed scheme with hybridization [21, 1].

Last step: the final scheme. Set

$$J_i = J_p^h(x_i), \quad p_i = p^h(x_i), \quad z_i = z^h(x_i), \quad V_i = V(x_i), \quad i = 0, \dots, N.$$

We will approximate the integrals in (3.12) and (3.13). Choose $\varphi = 1$ in I_i , $\varphi = 0$ elsewhere. Then we get from (3.13)

$$J_p^h(x_i) - J_p^h(x_{i-1}) = \int_{I_i} (J_p^h)_x = - \int_{I_i} f_k.$$

Approximating the integral on the right hand side by $-hf_k(x_{i-1})$, we see that

$$\frac{p_i^{j+1} - p_{i-1}^j}{k} + \frac{1}{h} (J_{p,i}^j - J_{p,i-1}^j) = 0.$$

We approximate $J_p^h \simeq J_i$ in I_i ; then, since V_x is constant in I_i , the integral in (3.12) can be computed if we take $\tau = 1$ in I_i , $\tau = 0$ elsewhere. Thus from

$$\int_{I_i} \frac{1}{r_i} e^{V/r_i} J_i + p_i e^{V/r_i} - p_{i-1} e^{V_{i-1}/r_i} = 0$$

It follows

$$J_i = - \left(\frac{V_i - V_{i-1}}{2} \coth \frac{V_i - V_{i-1}}{2r_i} \right) \frac{p_i - p_{i-1}}{h} - \frac{p_i + p_{i-1}}{2} \frac{V_i - V_{i-1}}{h} \quad \text{if } r_i > 0 \quad (3.15)$$

and $J_i = 0$ if $r_i = 0$. The discretization (3.15) can be seen as a nonlinear Scharfetter-Gummel scheme [22, 4], the nonlinearity being taken care of by the coefficient r_i .

The final scheme is the following: Given the boundary conditions $V_0^j, V_N^j \in \mathbb{R}$, $p_0^j, p_N^j, n_0^j, n_N^j \geq 0$ ($j > 0$) and initial conditions $(p_i^0)_{i=0}^N, (n_i^0)_{i=0}^N \in \mathbb{R}^{N+1}$, solve for $j \geq 0$, $1 \leq i \leq N-1$:

$$\frac{n_i^{j+1} - n_i^j}{k} - \frac{1}{h} (J_{n,i+1}^j - J_{n,i}^j) = 0, \quad (3.16)$$

$$\frac{p_i^{j+1} - p_i^j}{k} + \frac{1}{h} (J_{p,i+1}^j - J_{p,i}^j) = 0, \quad (3.17)$$

$$- \frac{V_{i+1}^j + 2V_i^j - V_{i-1}^j}{h^2} = n_i^j - p_i^j - C(x_i), \quad (3.18)$$

where

$$J_{n,i}^j = \left(\frac{V_i^j - V_{i-1}^j}{2} \coth \frac{V_i^j - V_{i-1}^j}{2\tilde{r}_i} \right) \frac{n_i^j - n_{i-1}^j}{h} - \frac{n_i^j + n_{i-1}^j}{2} \frac{V_i^j - V_{i-1}^j}{h},$$

$$J_{p,i}^j = - \left(\frac{V_i^j - V_{i-1}^j}{2} \coth \frac{V_i^j - V_{i-1}^j}{2\tilde{r}_i} \right) \frac{p_i^j - p_{i-1}^j}{h} - \frac{p_i^j + p_{i-1}^j}{2} \frac{V_i^j - V_{i-1}^j}{h},$$

if $r_i > 0$, $\tilde{r}_i > 0$, resp., and

$$J_{n,i}^j = 0,$$

$$J_{p,i}^j = 0,$$

if $r_i = 0$, $\tilde{r}_i = 0$, resp., \tilde{r}_i is defined by

$$\tilde{r}_i = \begin{cases} r'(n_{i-1}^j) & \text{if } \bar{J}_{n,i}^j \leq 0 \\ r'(n_i^j) & \text{if } \bar{J}_{n,i}^j > 0, \end{cases}$$

where

$$\bar{J}_{n,i}^j = \begin{cases} 0 & \text{if } n_i^j = n_{i-1}^j = 0 \\ \frac{\alpha}{\alpha-1} ((n_i^j)^{\alpha-1} - (n_{i-1}^j)^{\alpha-1}) - (V_i^j - V_{i-1}^j) & \text{else,} \end{cases}$$

and r_i is defined in (3.5) ($j \geq 0$, $1 \leq i \leq N$).

4. Numerical results

4.1. Due to the nonlinear diffusion terms $\nabla r(n) = \nabla(n^\alpha)$, $\nabla r(p) = \nabla(p^\alpha)$ it is possible that there are solutions n, p vanishing on parts of the semiconductor domain (cf. porous media equation). In [28] and [10] it is shown that indeed nonempty vacuum sets $\{n = 0\}$, $\{p = 0\}$ exist (in the a.e. sense) if the semiconductor is in thermal equilibrium. The non-stationary densities n, p to the contrary remain positive if the initial and boundary data are positive and the recombination rate satisfies some structural assumptions [12]. In this Section we present numerical examples showing transient vacuum solutions.

We are mainly interested in the following (physically motivated) situation: Start with arbitrary initial data and prescribe boundary data which are in thermal equilibrium. We expect that a solution of the transient problem converges to the solution of the thermal equilibrium state as $t \rightarrow \infty$.

4.2. Before presenting the numerical results we define the equilibrium state. The system (2.1)–(2.7) is said to be *in thermal equilibrium* if the electron and the hole current and the recombination rate vanish, i.e. $(n, p, V) \in (L^\infty(I))^3$ with $r(n), r(p), V \in H^1(I)$ is a *thermal equilibrium solution* if

$$J_n = r(n)_x - nV_x = 0, \quad (4.1)$$

$$J_p = -r(p)_x - pV_x = 0, \quad (4.2)$$

$$V_{xx} = n - p - C \quad \text{in } I, \quad (4.3)$$

$$n = n_D, \quad p = p_D, \quad V = V_D \quad \text{on } \partial I, \quad (4.4)$$

where n_D , p_D , V_D are defined in 2.1. It is well known [20] that the problem (4.1)–(4.4) admits a (generally nonunique) solution which is unique if in addition

$$h(n) - V \begin{cases} = h(n_i) & \text{if } n > 0 \\ \geq h(n_i) & \text{if } n = 0, \end{cases} \quad h(p) + V \begin{cases} = h(n_i) & \text{if } p > 0 \\ \geq h(n_i) & \text{if } p = 0 \end{cases} \quad (4)$$

hold. Here h is the enthalpy function defined by

$$h(s) \stackrel{\text{def}}{=} \int_1^s \frac{r'(\tau)}{\tau} d\tau, \quad s > 0,$$

and $n_i > 0$ is the intrinsic density. From (4.5) follows that (n_D, p_D, n_i) has to satisfy on ∂I the compatibility relation

$$h(n_D) + h(p_D) \begin{cases} = 2h(n_i) & \text{if } n_D p_D > 0 \\ \geq 2h(n_i) & \text{else.} \end{cases}$$

V_D has to satisfy (4.5). In this case we say that the boundary datum (n_D, p_D, V_D) is in *thermal equilibrium*.

The solution of (4.1)–(4.5) is the physically relevant solution (in the set of solutions of (4.1)–(4.4)) which minimizes the total energy of the system if the total number of electrons and holes in the device are prescribed [27].

Assume that $h(0+) > -\infty$, $h(\infty) = \infty$ (which is satisfied if $r(s) = s^\alpha$, $\alpha > 1$) and define the generalized inverse g of h

$$g(t) = \begin{cases} h^{-1}(t) & \text{if } h(0+) < t < \infty \\ 0 & \text{if } t \leq h(0+). \end{cases}$$

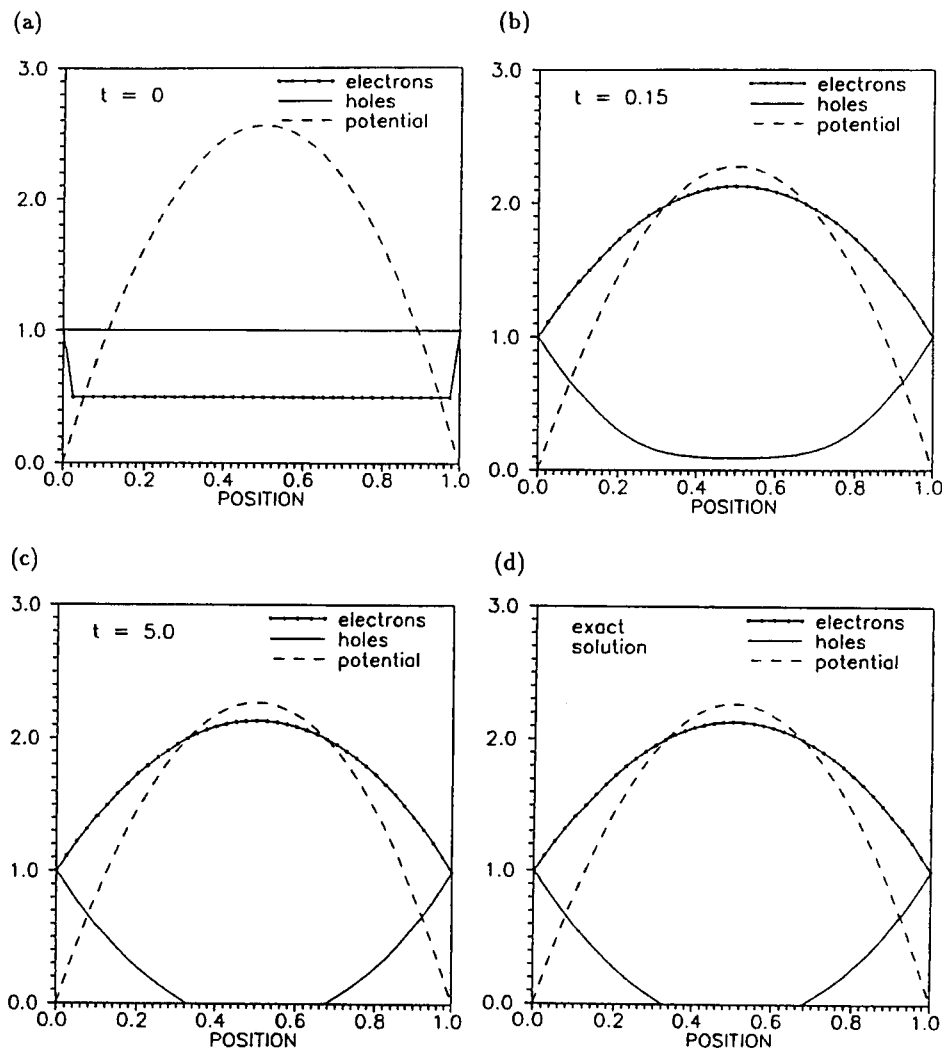


Fig. 1. Positive initial and boundary data. (a)–(c) Transient solutions, (d) exact equilibrium solution. At $t = 5.0$ the system is very close to the equilibrium state.

Since (4.5) is equivalent to $n = g(h(n_i) + V)$, $p = g(h(n_i) - V)$, (4.1)–(4.5) is equivalent to

$$V_{xx} = g(h(n_i) + V) - g(h(n_i) - V) - C \quad \text{in } I, \quad (4.6)$$

$$V = V_D \quad \text{on } \partial I, \quad (4.7)$$

$$n = g(h(n_i) + V), \quad p = g(h(n_i) - V) \quad \text{in } I. \quad (4.8)$$

In the following we assume that

$$r(s) = s^\alpha, \quad s \geq 0, \quad \alpha > 1.$$

4.3. Positive initial and boundary data. As a first example we take nonvanishing initial and boundary data, a constant doping profile $C = 20$, and a pressure coefficient $\alpha = 2$ (Fig. 1a). For all example, the length of the interval is $l = 1$ and the mesh size is $h = 0.025$. Note that the boundary data

$$n(0) = n(1) = p(0) = p(1) = 1, \quad V(0) = V(1) = 0$$

are in thermal equilibrium. From Prop. 4.2 in [11] it is known that the densities are positive in $I \times (0, \infty)$ (Fig. 1b). The solution converges to the equilibrium state as $t \rightarrow \infty$ (Fig. 1c). This can be seen as follows. Since $\alpha = 2$, $g(t) = (\frac{1}{2}t + 1)_+ = \max(0, \frac{1}{2}t + 1)$, and $n > 0$, $p > 0$ in $I \times (0, \infty)$, (4.6)–(4.7) is a linear boundary value problem for V which can be solved explicitly. The equilibrium densities n, p can be computed from (4.8). In Fig. 1d the exact equilibrium solution is plotted which is equal to the steady state solution in Fig. 1c.

Note that the vacuum sets are empty as long as $t < \infty$, but nonempty in the limit $t \rightarrow \infty$.

Positive boundary data, nonnegative initial data. We take the same boundary conditions as in the first example but the initial data vanish on subintervals (Fig. 2a). Again, $C = 20$, $\alpha = 2$. After the finite time $t_0 > 0$ the densities become positive for all $t \geq t_0$ (Fig. 2b, c); in the limit $t \rightarrow \infty$ the system reaches the equilibrium state (Fig. 2d).

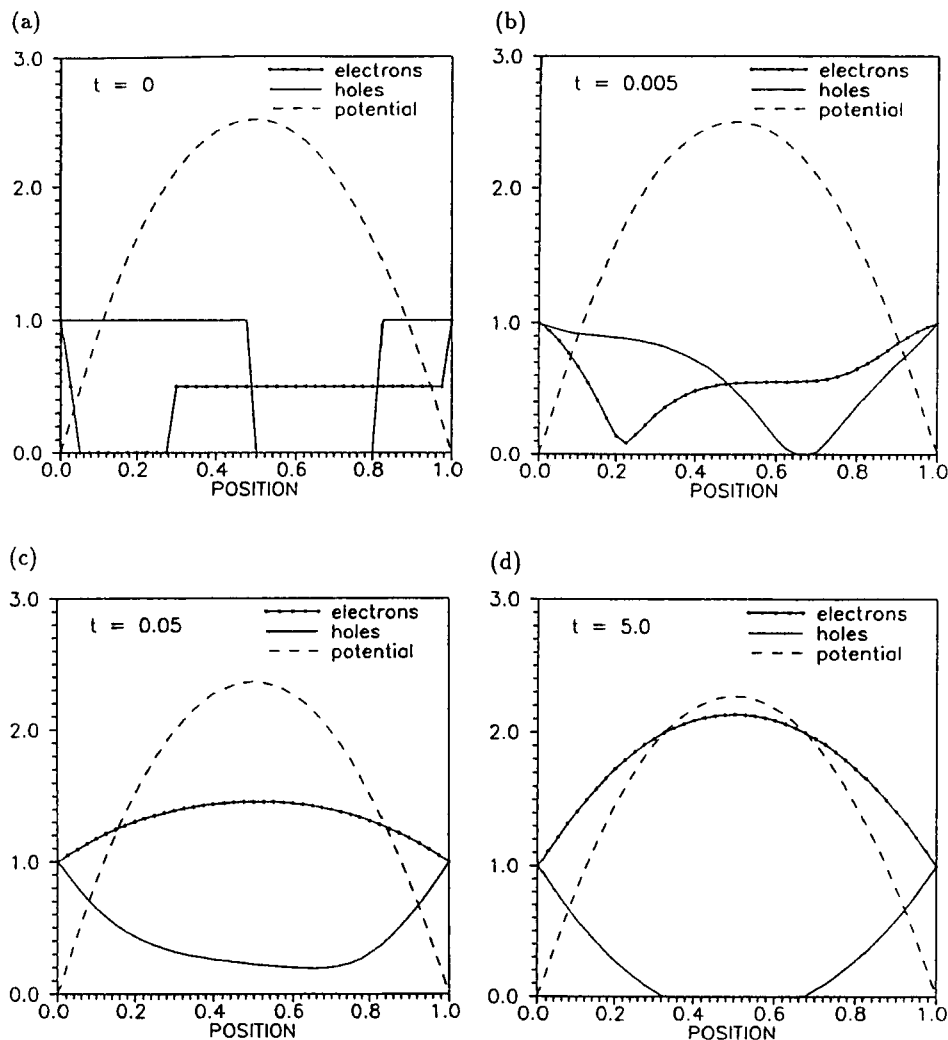


Fig. 2. Nonnegative initial data, positive boundary data. (a)–(d) Transient solutions; at $t = 5.0$ the system is very close to the equilibrium state.

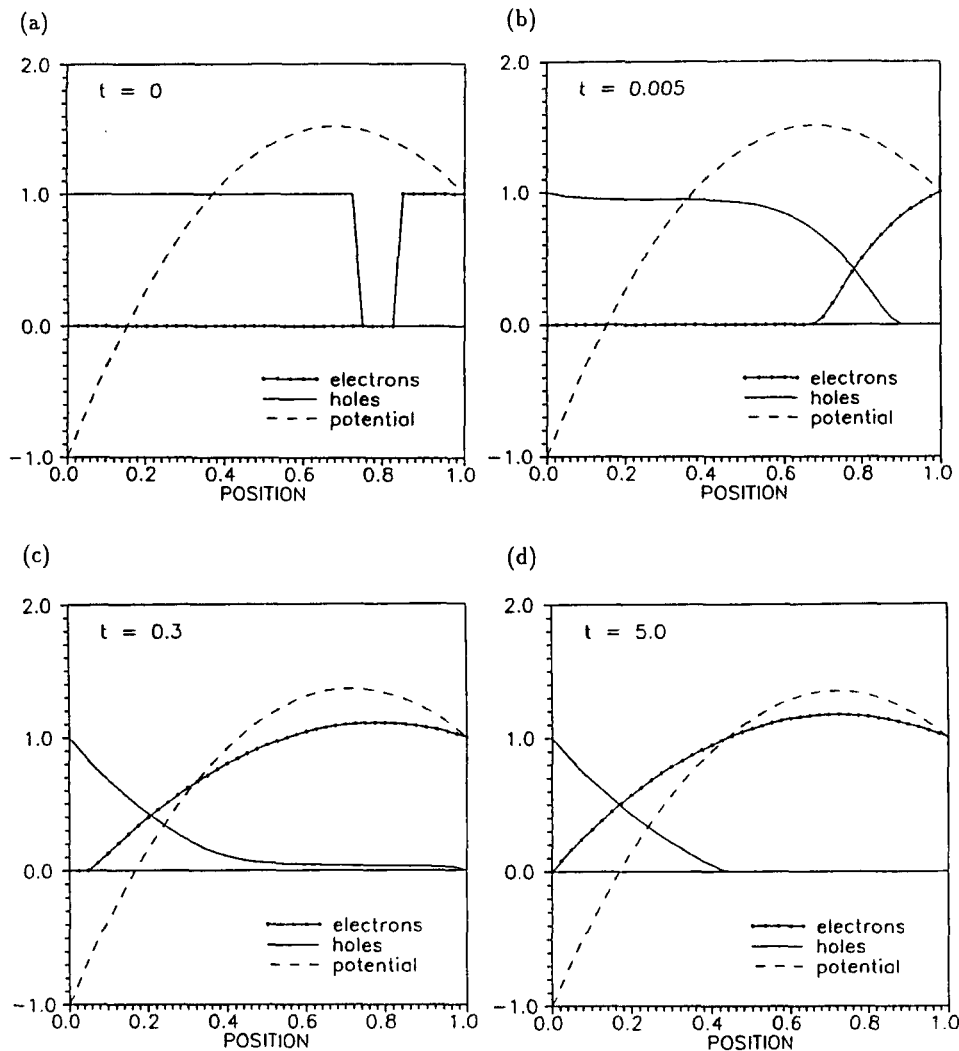


Fig. 3. Nonnegative initial data and boundary data. (a)–(d) Transient solutions; at $t = 5.0$ the system is very close to equilibrium state.

Nonnegative initial and boundary data. In this example we choose the (equilibrium) boundary data

$$n(0) = p(1) = 0, \quad n(1) = p(0) = 1, \quad V(0) = -1, \quad V(1) = 1,$$

$C = 10$, $\alpha = 2$, and the initial data as shown in Fig. 3a. As in the preceding example we observe that the densities become positive after the time $t_0 > 0$ (Fig. 3b, c). At $t = 5$ the system is very close to the equilibrium state (Fig. 3d) which admits a nonempty vacuum set $\{p = 0\}$.

It seems that vacuum sets can only occur for short time (if the initial data vanish partly) and in the limit $t \rightarrow \infty$ provided that the equilibrium state has vacuum densities. The example of a diode in the next Section shows, however, that the non-equilibrium state admits vacuum solutions for all $t \geq 0$.

4.4 If the mesh size h tends to zero, we expect that the approximate stationary solution (n^h, p^h, V^h) obtained from (3.16)–(3.18) in the limit $j \rightarrow \infty$ converges in some topology (e.g. $(L^2(I))^3$) to the corresponding exact stationary solution of (2.1)–(2.7). It would be out of place to prove this analytically here, but we present an example which makes plausible the convergence of the approximate solution and we compute the orders of convergence. Take $\alpha = 5/3$,

$$C(x) = \begin{cases} -30 & \text{if } 0 < x \leq 0.7 \\ 80 & \text{if } 0.7 < x < 1, \end{cases}$$

and the boundary data

$$n(0) = p(1) = 0, \quad n(1) = p(0) = 1, \quad V(0) = -\frac{5}{4}, \quad V(1) = -\frac{5}{4} - U,$$

with $U = 4$. This model can be interpreted as a (simple) forward biased PN diode (see Section 5). Since no exact solution is available we take the stationary solution (n^*, p^*, V^*) with “small” mesh size $h^* = 1/640$ as “exact” solution. Set

$$E_u(h) = \|u^h - u^*\|_{L^2(I)}$$

Table 4.1

h	$\ p^h - p^*\ _{L^2}$	β	$\ n^h - n^*\ _{L^2}$	β	$\ V^h - V^*\ _{L^2}$	β
1/10	0.2685		0.2812		0.6115	
1/20	0.1388	0.95	0.1316	1.10	0.2999	1.03
1/40	0.0680	1.03	0.0605	1.12	0.1452	1.05
1/80	0.0318	1.10	0.0281	1.11	0.0677	1.10

for $u = n, p, V$. Then from the (assumed) relation $E_u(h) = kh^\beta$ with $\beta > 0$ and k independent of h , it follows that by computing two discrete solutions with two different parameters h_1, h_2 , the order of convergence is equal to

$$\beta = \frac{\log(E_u(h_1)/E_u(h_2))}{\log(h_1/h_2)}.$$

The error in L^2 shown in Table 4.1 for various values of h appears to be $O(h)$. For a linear elliptic problem with H^2 solution the L^2 error is $O(h^2)$ [6]. Generally this accuracy cannot be expected here since the stationary solutions are generally not in H^2 .

5. The PN junction diode

5.1. A PN junction diode consists of a region where the preconcentration of negative ions dominates ($C(x) < 0$), the P-region, and a region where the preconcentration of positive ions dominates ($C(x) > 0$), the N-region. In order to model the device accurately, we solve numerically the drift-diffusion model including the physical parameters.

We consider the equations (1.1)–(1.3) neglecting recombination-generation effects subject to the boundary conditions

$$n = n_D, \quad p = p_D, \quad V = V_D + V_a \quad \text{on } \partial I, \quad t \geq 0,$$

and initial conditions

$$n = n_I, \quad p = p_I \quad \text{in } I, \quad t = 0.$$

V_a is the applied potential, at the anode $V_a(0) = 0$, at the cathode $V_a(l) = -U$. We assume that the boundary datum (n_D, p_D, V_D) is in thermal equilibrium. (n_D, p_D, V_D) is derived from a slightly different consideration as in the previous Section. We require additionally that the space charge vanishes at the Ohmic contacts. Thus, given $n_i > 0$ and $C(x)$, let $n_D(x), p_D(x) \geq 0$ on ∂I be the (unique) solution of

$$n_D - p_D - C = 0, \tag{5.1}$$

$$h(n_D) + h(p_D) \begin{cases} = 2h(n_i) & \text{if } n_D p_D > 0 \\ \geq 2h(n_i) & \text{else.} \end{cases} \tag{5.2}$$

h is the enthalpy function defined in 4.2. In applications the doping profile is nearly constant near the contacts, thus $C(0), C(l)$ make sense. Now the equilibrium boundary potential can be derived using n_D, p_D :

$$V_D = \begin{cases} \frac{D_n}{\mu_n} (h(n_D) - h(n_i)) & \text{if } n_D > 0, \quad p_D \geq 0, \\ \frac{D_p}{\mu_p} (h(n_i) - h(p_D)) & \text{if } n_D = 0, \quad p_D > 0, \\ 0 & \text{if } n_D = 0, \quad p_D = 0. \end{cases} \tag{5.3}$$

Furthermore, we assume that the system is in thermal equilibrium at $t = 0$, i.e. $U(0) = 0$, and n_I, p_I solve (4.6)–(4.8) (including the parameters).

5.2. We impose the following assumptions on the physical parameters:

- (1) The pressure is given by $r(s) = s^\alpha$, $s \geq 0$, $\alpha > 1$.
- (2) The permittivity ε is constant throughout the device.
- (3) The diffusion constants $D \stackrel{\text{def}}{=} D_n = D_p$ and mobilities $\mu \stackrel{\text{def}}{=} \mu_n = \mu_p$ are constant throughout the semiconductor.
- (4) The doping profile C is given with abrupt junction

$$C(x) = \begin{cases} -c_0 & \text{if } 0 < x < l_0 \\ c_1 & \text{if } l_0 < x < l, \end{cases}$$

where

$$c_1 \geq c_0 > g(2h(n_i)) = 2^{1/(\alpha-1)} n_i > 0.$$

Whereas the second hypothesis is generally accepted for isotropic and homogeneous materials [24, Ch. 1], the third assumption is only valid approximately, but simplifies the computations below.

Generally, D_n and D_p , μ_n and μ_p differ, and the mobilities depend on C , $|V_x|$, and the material (see [24, Ch. 1], p. 791)). In practise the doping profile varies extremely fast close to the junction where C changes sign while it varies slowly away from the junction, and the absolute values of the concentrations are much larger than n_i ; therefore the last assumption seems physically reasonable.

5.3. In the standard drift-diffusion model (with linear pressure) the diffusion coefficients are derived from the Einstein relation

$$D_n = U_T \mu_n, \quad D_p = U_T \mu_p, \quad (5.5)$$

where $U_T = k_B T/q$ is the thermal voltage and k_B the Boltzmann constant. These expressions follow from the equations (1.1)–(1.2) in the thermal equilibrium case $J_n = J_p = 0$ and the Maxwellian form of the equilibrium densities n_e, p_e [Ch. 26]. In Section 4 we have shown that n_e, p_e are not given as exponential functions of the equilibrium potential V_e . Therefore we cannot expect that (5.5) holds in our model. We compute the diffusion constant by the following consideration:

From (5.1)–(5.3) and assumption (4) follow:

$$\begin{aligned} n_e(0) = p_e(l) = 0, \quad n_e(l) = c_1, \quad p_e(0) = c_0, \\ V_e(0) = \frac{\gamma D}{\mu} (n_i^{\alpha-1} - c_0^{\alpha-1}), \quad V_e(l) = \frac{\gamma D}{\mu} (c_1^{\alpha-1} - n_i^{\alpha-1}), \end{aligned}$$

where we have set

$$\gamma = \frac{\alpha}{\alpha - 1} > 1.$$

The barrier or diffusion potential V_b (also called *built-in potential*) can be obtained from measurements and is given by $V_b = V_e(l) - V_e(0)$. Using V_b the diffusion constant can be computed as

$$D = \frac{\mu V_b}{\gamma(c_0^{\alpha-1} + c_1^{\alpha-1} - 2n_i^{\alpha-1})}. \quad (5.6)$$

This expression is consistent with the Einstein relations in the sense that (5.6) coincides with (5.5) as $\alpha \rightarrow 1$. Indeed, since

$$\gamma(c_0^{\alpha-1} + c_1^{\alpha-1} - 2n_i^{\alpha-1}) \rightarrow \ln \frac{c_0 c_1}{n_i^2} \quad (\alpha \rightarrow 1)$$

and

$$V_b = \frac{k_B T}{q} \ln \frac{c_0 c_1}{n_i^2},$$

if $\alpha = 1$ [24, Ch. 2.3.1] we get

$$D \rightarrow \frac{k_B T}{q} \mu = U_T \mu \quad (\alpha \rightarrow 1).$$

The numerical values for the parameters (for a one-dimensional silicon diode) are given in Table 5.1. Note that all these data can be obtained from measurement.

Table 5.1

parameter	physical meaning	numerical value
q	elementary charge	10^{-19} As
ϵ	permittivity constant	10^{-12} As V ⁻¹ cm
n_i	intrinsic number	10^{10} cm ⁻³
l	device length	10^{-3} cm
μ	mobility	10^3 cm ² V ⁻¹ s ⁻¹
V_b	barrier potential	0.8 V
$ C $	moderate doping concentration	10^{15} cm ⁻³

5.4. Now we bring the equations (1.1)–(1.3) into an appropriate scaled and dimensionless form. The scaling is as follows (see also [16, 15]):

$$C = c_1 C_s, \quad n = c_1 n_s, \quad p = c_1 p_s, \quad V = (V_b U_0) V_s, \quad x = l x_s, \quad t = \tau t_s,$$

where

$$U_0 = \frac{1}{\gamma(1 + \eta - 2\delta)}, \quad \tau = \frac{l^2}{\mu V_b},$$

and $\eta = (c_0/c_1)^{\alpha-1}$, $\delta = (n_i/c_1)^{\alpha-1}$. Set

$$\lambda^2 = \frac{\varepsilon V_b U_0}{q l^2 c_1}.$$

Keeping the same notation of all variables, the doping profile, and U_0 we get

$$n_t - U_0((n^\alpha)_x - n V_x)_x = 0, \quad (5.7)$$

$$p_t - U_0((p^\alpha)_x + p V_x)_x = 0, \quad (5.8)$$

$$\lambda^2 V_{xx} = n - p - C \quad \text{in } (0, 1) \times (0, T), \quad (5.9)$$

$$n(0, t) = p(1, t) = 0, \quad n(1, t) = 1, \quad p(0, t) = \eta^{\gamma-1}, \quad (5.10)$$

$$V(0, t) = -\gamma(1 - \delta), \quad V(1, t) = \gamma(1 - \delta) - U, \quad t \in (0, T), \quad (5.11)$$

$$n(x, 0) = n_e(x), \quad p(x, 0) = p_e(x), \quad x \in (0, 1), \quad (5.12)$$

and (n_e, p_e) is the solution of

$$\lambda^2 V_{xx} = n_e - p_x - C \quad \text{in } (0, 1), \quad (5.13)$$

$$V(0) = -\gamma(1 - \delta), \quad V(1) = \gamma(1 - \delta), \quad (5.14)$$

$$n_e = (\delta + \gamma^{-1} V)_+^{\gamma-1}, \quad p_e = \eta^{\gamma-1} (\delta - \gamma^{-1} V)_+^{\gamma-1} \quad \text{in } (0, 1). \quad (5.15)$$

Note that we get, as $\alpha \rightarrow 1$, the scaling of [15]. The currents can be computed from the scaled currents $J_{n,s} = U_0((n^\alpha)_x - n_s(V_s)_x)$, $J_{p,s} = -U_0((p^\alpha)_x + p_s(V_s)_x)$ as follows:

$$J_n = \frac{q \mu c_1 V_b}{l} J_{n,s}, \quad J_p = \frac{q \mu c_1 V_b}{l} J_{p,s}. \quad (5.16)$$

5.5. We present examples of stationary states for different applied voltages. We take a moderately doped silicon diode with

$$c_0 = c_1 = 10^{15} \text{ cm}^{-3}, \quad l = 10^{-3} \text{ cm}, \quad l_0 = 0.7 \cdot 10^{-3} \text{ cm}$$

(see assumption (4)) with n_i , μ , and V_b as in Table 5.1. Let (n_e, p_e, V_e) be the equilibrium solution of (5.13)–(5.15). Since

$$V_e(0) < -\gamma\delta, \quad V_e(1) > \gamma\delta,$$

and V_e is continuous in $[0, 1]$, there exist $x_n, x_p \in (0, 1)$ such that $V < -\gamma\delta$ in $[0, x_n]$, $V > \gamma\delta$ in $[x_p, 1]$ which implies that there are nontrivial vacuum sets

$$\{n_e = 0\} = [0, x], \quad \{p_e = 0\} = [x_p, 1]. \quad (5.17)$$

(From a maximum principle argument it can be seen that V_e is increasing in (x_n, x_p) , hence we have equality in (5.17).) The equilibrium solution is shown in Fig. 4a. In Fig. 4b the stationary densities and the potential for the reverse (unscaled) bias $U = -0.8$ V are depicted. The vacuum sets are larger than in equilibrium and no current flows. This is also the case if a slightly forward bias $U = 0.35$ V is applied (Fig. 4c), whereas for $U = 1.0$ V the vacuum sets are trivial (Fig. 4d).

In thermal equilibrium the sum of the hole diffusion current $-(p^\alpha)_x$ and the drift current $-p V_x$ is zero. When $U < 0$ we expect (but cannot prove analytically) that for $t > 0$ the electric field $|V_x(x, t)|$ is larger than $|V_x(x, 0)|$ near the junction. Thus drift current dominates and the holes flow in the direction of the anode $x = 0$ until reaching the steady state. Therefore, there is vacuum for all $t > 0$ in the reverse bias case. Numerically it turns out that vacuum for all time $t > 0$ occurs if $U \in (-\infty, U_{th})$ where $U_{th} \simeq 0.4$ V is called threshold voltage. In the next Section we show numerically that current flows if $U > U_{th}$.

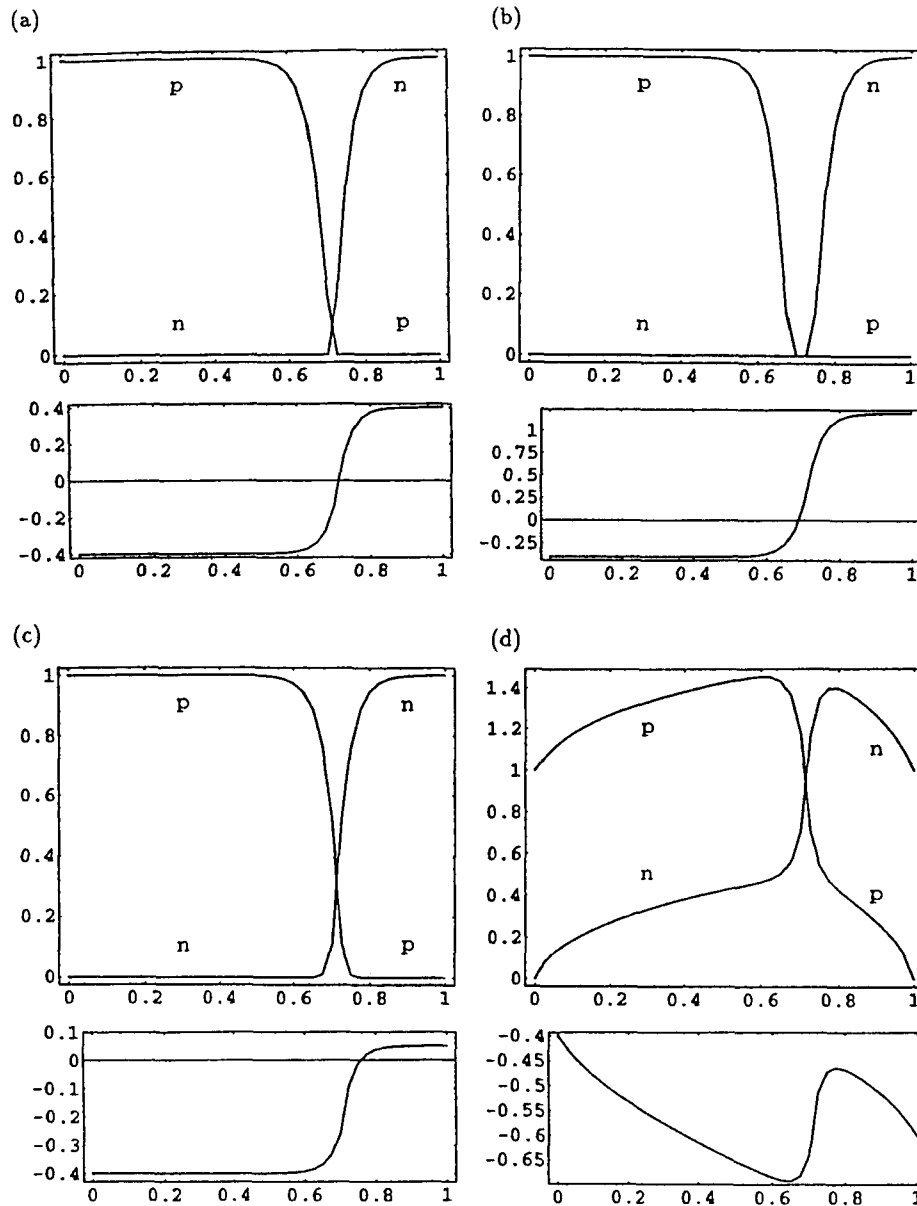


Fig. 4. Carrier densities (in 10^{15} cm^{-1}) and potential (in V) of a Si diode depending on the position (in 10^{-3} cm). (a) Thermal equilibrium $U = 0$, (b) reverse bias $U = -1.6 \text{ V}$, (c) forward bias $U = 0.35 \text{ V}$, (d) forward bias $U = 1 \text{ V}$

6. Static voltage-current characteristics

In the preceding Section we have found that due to the vacuum effect, no current can flow in the reverse and slightly forward biased case. In this Section we compute numerically voltage-current characteristics of a diode (i.e. dependences of the current on the applied voltage) and discuss the differences of these characteristics to characteristics of a real diode.

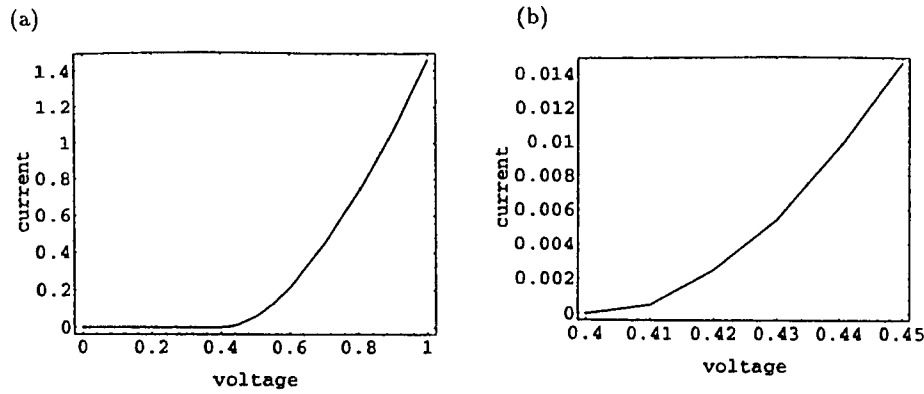
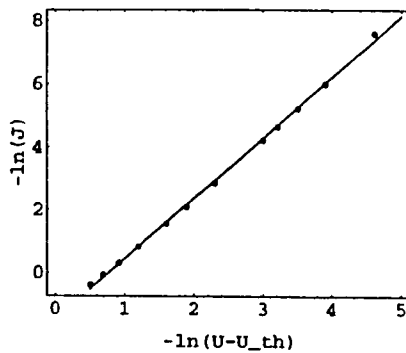
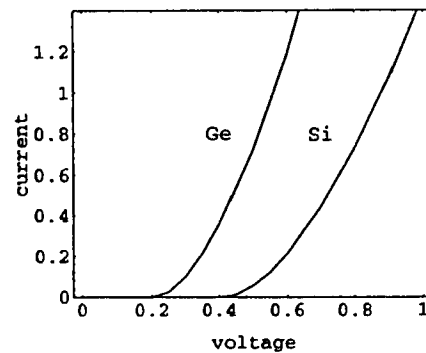
6.1. Characteristic of a silicon diode. The voltage-current characteristic of a Si diode with the same data as in 5.5 is depicted in Fig. 5. For $U \in (-\infty, 0.4 \text{ V})$ the total current $J = J_n + J_p$ vanishes; for $U > 0.4 \text{ V}$ a positive current flows (and there is no vacuum in $(0, 1)$). The maximal voltage where no current flows is called *threshold voltage* U_{th} (see Fig 5). The dependence of the current on the applied voltage takes the form (cf. Fig. 6)

$$J = J_s(U - U_{th})^\beta, \quad \beta = 1.9 \pm 0.2 \quad (U \geq U_{th}).$$

As shown in Table 6.1, the value for U_{th} seems not to depend on the size of the P-region with respect to the N-region denoted by l_0/l .

In Fig. 7 the characteristics of a Ge and Si diode are shown. The Ge diode has the same length and doping concentration as the Si diode but

$$n_i = 10^{13} \text{ cm}^{-1}, \quad V_b = 0.4 \text{ V}$$

Fig. 5. Characteristic of a Si diode (U in V, J in $40 \mu\text{A}$). (a) Full characteristic, (b) detailFig. 6. Logarithmic plot of Fig. 5a ($U_{th} = 0.40 \text{ V}$)Fig. 7. Characteristic of a Ge and Si diode (U in V, J in $40 \mu\text{A}$)

(see [24, p. 76], [8, Ch. 1]). For simplicity we take $\mu = 10^3 \text{ cm}^3 \text{ V}^{-1} \text{ s}^{-1}$ and $\varepsilon = 10^{-12} \text{ As V}^{-1} \text{ cm}$. We obtain $U_{th} \simeq 0.20 \text{ V}$ and

$$J = J_s(U - U_{th})^\beta, \quad \beta = 1.4 \pm 0.3.$$

We conjecture that

$$U_{th} \simeq \frac{V_b}{2}$$

(provided that $\delta \ll 1$).

6.2. Dependence on C and α . When the Si diode is less doped than in 6.1, there are less carriers and we expect a smaller current. This behaviour is shown in Fig. 8 for the doping impurity $c_0 = c_1 = 10^{13} \text{ cm}^{-3}$. In Fig. 9 the dependence of the current on the pressure coefficient α is depicted. It turns out that again we have

$$J = J_s(U - U_{th})^\beta$$

and β increases as $\alpha > 1$ decreases (see Table 6.2). This is expected since the growth for $\alpha = 1$ is exponential (at least for “small” U , cf. (1.7)). For $\alpha \in \{1.1, 5/3, 2.5\}$ we get $U_{th} \simeq 0.4 \text{ V}$.

Table 6.1

l_0/l	$U_{th} \text{ (V)}$
0.2	0.39 ... 0.40
0.5	0.40 ... 0.41
0.7	0.40 ... 0.41
0.9	0.39 ... 0.40

Table 6.2

α	β
1.1	5.3 ± 0.3
5/3	1.9 ± 0.2
2.5	1.3 ± 0.2

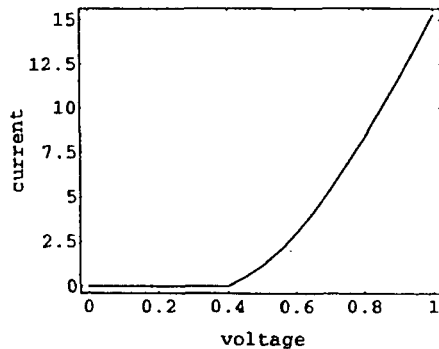


Fig. 8. Characteristic of a Si diode with $c_0 = c_1 = 10^{13} \text{ cm}^{-3}$ (U in V, J in 40 nA)

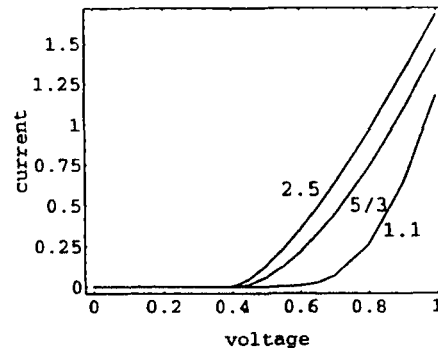


Fig. 9. Characteristics for $\alpha = 2.5, \alpha = 5/3, \alpha = 1.1$ (U in V, J in 40 μA)

6.3. Discussion of the results. We compare the numerical results with the characteristic of a practical Si diode. In the forward direction, for applied voltages which are of the same order as the thermal voltage $U_T \approx 0.026 \text{ V}$ (at $T = 300 \text{ K}$), the experimental results can be in general represented by the empirical form $J = J_s(\exp(U/2U_T) - 1)$ [24, p. 91]. The current is mainly a recombination current. When U is larger, for example several U_T , the diffusion current dominates and the Shockley equation $J = J_s(\exp(U/U_T) - 1)$ is valid. For these voltages the current is very small (several μA or nA depending on the doping; cf. [24, p. 91], [23, p. 20]) compared to the maximally admissible current. In our model the current in the slightly forward direction vanishes.

At high injection conditions, when U is larger than the built-in potential $V_b = U_T \cdot \ln(c_0 c_1 / n_i^2) = (10 \ln 10) U_T$ (for $c_0 = c_1 = 10^{15} \text{ cm}^{-3}$ and $\alpha = 1$) the growth of the characteristic slows down. In [24, p. 94] the current becomes roughly proportional to $(\exp(U/2U_T) - 1)$, MARKOWICH et al. [19, p. 191f.] obtain the relation $I \sim U^2$. We also get a polynomial growth. The voltage at which the characteristic slows down is called threshold voltage U_{th} (cf. [25, p. 26ff.]). The experimental values for a Si and Ge diode are $U_{th} \approx 0.5 \text{ V}$, $U_{th} \approx 0.2 \text{ V}$ resp. [25, p. 26ff.] which is of the same order as our results.

In the reverse biased case a small leakage current flows which is a generation current for Si diodes. The Shockley equation qualitatively predicts this behaviour. The current is small (of order $1 \text{ nA} \dots 1 \mu\text{A}$ depending on the diode, cf. [25]); we obtain vanishing current.

We can conclude that the drift-diffusion model with nonlinear diffusion qualitatively predicts the voltage-current characteristic and threshold voltage of Si diodes under high injection conditions.

6.4. Additional remarks. Due to the simplifications we can only expect to obtain qualitative agreement with the experimental data. To get better results we have to include e.g. the dependence of the mobilities on the doping and the material (see assumption (3) in 5.2) and the recombination-generation rate R . In regions where the carrier densities fall short of their equilibrium values as a consequence of a reverse bias, generation occurs faster than recombination, thus $R \leq 0$. The function $-R(n, p)$ on the right hand side of (1.1)–(1.2) therefore represents a “source” of carriers and a generation current is expected to flow. But yet no physically reasonable model for R is known.

It is uncertain whether vanishing carrier densities really occur in practical semiconductors. The pressure $r(s) = c_0 s + c_1 s^\alpha$ ($\alpha > 1$) can be tried as another model. Then the equations (1.1)–(1.2) are uniformly parabolic and existence and uniqueness of the mathematical model are known (see [11]). In this model we conjecture that $n > 0$, $p > 0$ holds (cf. [9]). If the scaled densities n, p are small compared to one the first term $c_0 s$ is dominant; in the high injection regime where n, p are larger than one the second term $c_1 s^\alpha$ is dominant. Possibly this function models a diode in the low injection as well as in the high injection case.

Physically a three- or even two-dimensional domain gives a better model than a one-dimensional interval. Since in higher dimensions the computing times goes up it should be better to treat the stationary equations directly using the mixed exponential fitting method like in Section 3. In BREZZI et al. [5] the one-dimensional Scharfetter-Gummel method for the standard model is generalized to two-dimensional problems.

Acknowledgement: A part of this work was made at the Department of Mathematics, Arizona State University, in Tempe (USA). It is a pleasure to thank C. RINGHOFER for his invitation and stimulating discussions. Furthermore, I am grateful to P. PIETRA for the hint to the paper [1] and useful discussions.

This work was partially supported by the EC-network, contract # ERBCHRX-CT930-413 and by the DFG (Deutsche Forschungsgemeinschaft), MA1662/-1 and 2.

References

- 1 ARIMBURGO, F.; BAIocchi, C.; MARINI, L.: Numerical approximation of the 1-D nonlinear drift-diffusion model in semiconductors. In BOFFI, V.; BAMPI, F.; TOSCANI, G. (eds.): Nonlinear kinetic theory and mathematical aspects of hyperbolic systems. World Scientific, Singapore 1992, pp. 1–10.
- 2 ASHCROFT, N.; MERMIN, N.: Solid state physics. Saunders College, Philadelphia 1976.

- 3 BÖER, K.: Survey of semiconductor physics. Van Nostrand Reinhold, New York 1990.
- 4 BREZZI, F.; MARINI, L.; PIETRA, P.: Méthodes d'éléments finis mixtes et schéma de Scharfetter-Gummel. C. R. Acad. Sci., Paris **305** (1987), 599–604.
- 5 BREZZI, F.; MARINI, L.; PIETRA, P.: Two-dimensional exponential fitting and applications to drift-diffusion models. SIAM J. Numer. Anal. **26** (1989), 1342–1355.
- 6 CIARLET, P.: The Finite Element Method for elliptic problems. North-Holland, Amsterdam 1978.
- 7 COURANT, R.; FRIEDRICHS, K. O.: Supersonic flow and shock waves. Interscience 1967.
- 8 FRASER, D.: The physics of semiconductor devices. Clarendon Press, 3rd edition, Oxford 1983.
- 9 GAJEWSKI, H.; GRÖGER, K.: Semiconductor equations for variable mobilities based on Boltzmann statistics or Fermi-Dirac statistics. Math. Nachr. **140** (1989), 7–36.
- 10 JÜNGEL, A.: The free boundary problem of a semiconductor in thermal equilibrium. (To appear in MMAS 1995).
- 11 JÜNGEL, A.: On the existence and uniqueness of transient solutions of a degenerate nonlinear drift-diffusion model for semiconductors. M³AS **4** (1994), 677–703.
- 12 JÜNGEL, A.: Qualitative behavior of transient solutions of a degenerate nonlinear drift-diffusion model for semiconductors. (To appear in M³AS 1995).
- 13 KALASHNIKOV, A. S.: Some problems of the qualitative theory of non-linear degenerate second-order parabolic equations. Russ. Math. Surveys **42** (1987), 169–222.
- 14 LADYZENSKAYA, O. A.; SOLONNIKOV, V. A.; URAL'CEVA, N. N.: Linear and quasilinear equations of parabolic type. Amer. Math. Soc., Providence 1968.
- 15 MARKOWICH, P.: A singular perturbation analysis of the fundamental semiconductor device equations. SIAM J. Appl. Math. **44** (1984), 898–928.
- 16 MARKOWICH, P.; RINGHOFER, C.: A singularly perturbed boundary value problem modelling a semiconductor device. SIAM J. Appl. Math. **44** (1984), 231–256.
- 17 MARKOWICH, P. A.: The stationary semiconductor device equations. Springer, Wien 1986.
- 18 MARKOWICH, P. A.: On steady state Euler-Poisson models for semiconductors. ZAMP **42** (1991), 385–407.
- 19 MARKOWICH, P. A.; RINGHOFER, C. A.; SCHMEISER, C.: Semiconductor equations. Springer, Berlin etc. 1990.
- 20 MARKOWICH, P. A.; UNTERREITER, A.: Vacuum solutions of the stationary drift-diffusion mode. Ann. Sc. Norm. Sup. di Pisa **20** (1993), 371–386.
- 21 RAVIART, P.; THOMAS, J.: A mixed finite element method for second order elliptic equations. In: Mathematical aspects of the Finite Element Method. Volume 606 of Lecture Notes in Math., Springer, Berlin etc. 1977, pp. 292–315.
- 22 SCHARFETTER, D.; GUMMEL, H.: Large signal analysis of a Silicon Read diode oscillator. IEEE Trans. El. Dev. **ED-16** (1969), 64–77.
- 23 SHAW, M.: Properties of junctions and barriers. In Moss, T. (ed.): Handbook on semiconductors. Volume 4. North-Holland, Amsterdam 1981, pp. 1–87.
- 24 SZE, S.: Physics of semiconductor devices. John Wiley, New York 1981.
- 25 THOLL, H.: Bauelemente der Halbleiterelektronik. Vol. 1. Teubner, Stuttgart 1976.
- 26 TROIANIELLO, G.: Elliptic differential equations and obstacle problems. Plenum Press, New York 1987.
- 27 UNTERREITER, A.: The thermal equilibrium states of semiconductor devices. Appl. Math. Lett. **7** (1994), 39–43.
- 28 UNTERREITER, A.: Vacuum and non-vacuum solutions of the quasi-hydrodynamic semiconductor model in thermal equilibrium. MMAS **18** (1995), 225–254.
- 29 ZLAMAL: Finite element solution of the fundamental equations of semiconductor devices. I. Math. Comput. **46** (1986), 27–43.

Received April 7, 1994, revised August 4, 1994, accepted October 10, 1994

Address: Dr. ANSGAR JÜNGEL, Technische Universität Berlin, FB Mathematik – Sekr. MA 6-3, Straße des 17. Juni 136, D-10623 Berlin, Germany